

High-field ESR studies of the quantum spin magnet CaCu_2O_3

M Goiran¹, M Costes¹, J M Broto¹, F C Chou^{2‡}, R Klingeler^{1,4}, E Arushanov^{1,3,4}, S-L Drechsler⁴, B Büchner⁴ and V Kataev⁴

¹Laboratoire National des Champs Magnétiques Pulsés, 31432 Toulouse Cedex 04, France

²Center for Materials Science and Engineering, Massachusetts Institute of Technology, Cambridge, Massachusetts 02139

³Institute of Applied Physics, Academy of Sciences of Moldova, MD 2028 Chisinau, Moldova

⁴Leibniz Institute for Solid State and Materials Research IFW Dresden, P.O. Box 270116, D-01171 Dresden, Germany

E-mail: goiran@lncmp.org and v.kataev@ifw-dresden.de

Abstract.

We report an electron spin resonance (ESR) study of the $s = 1/2$ -Heisenberg pseudo-ladder magnet CaCu_2O_3 in pulsed magnetic fields up to 40 T. At sub-Terahertz frequencies we observe an ESR signal originating from a small amount of uncompensated spins residing presumably at the imperfections of the strongly antiferromagnetically correlated host spin lattice. The data give evidence that these few percent of "extra" spin states are coupled strongly to the bulk spins and are involved in the antiferromagnetic ordering at $T_N = 25$ K. By mapping the frequency/resonance field diagram we have determined a small gap for magnetic excitations below T_N of the order of $\sim 0.3 - 0.8$ meV. Such a small value of the gap explains the occurrence of the spin-flop transition in CaCu_2O_3 at weak magnetic fields $\mu_0 H_{sf} \sim 3$ T. Qualitative changes of the ESR response with increasing the field strength give indications that strong magnetic fields reduce the antiferromagnetic correlations and may even suppress the long-range magnetic order in CaCu_2O_3 . ESR data support scenarios with a significant role of the "extra" spin states for the properties of low-dimensional quantum magnets.

PACS numbers: 71.27.+a, 76.30.Fc, 75.10.Jm

Submitted to: *New J. Phys.*

‡ Present address: Center of Condensed Matter Sciences, National Taiwan University, Taipei 106, Taiwan

1. Introduction

Imperfections in quasi-one- or two-dimensional spin lattices [1] may result in peculiar changes of the properties of low-dimensional quantum antiferromagnets. The host spin system around the defects such as nonmagnetic vacancies, doped "extra" spins or spin states at lattice edges is strongly disturbed which is particularly pronounced in the Heisenberg magnets comprising small spins (e.g. $s = 1/2$). A prominent example is the doping of a two-dimensional (2D) $s = 1/2$ Heisenberg antiferromagnet (HAF) with nonmagnetic impurities. Local magnetic moments associated with nonmagnetic Zn dopants in the CuO_2 planes of high temperature superconductors have been observed by a number of experimental techniques (see e.g. Ref. [2, 3, 4]) in accord with theoretical predictions [5, 6, 7, 8]. Another interesting aspect of imperfect spin lattices is the enhancement of antiferromagnetic correlations near impurities in low-D HAFs regardless the presence or absence of long range order in the ground state of the host [9, 10, 11]. Thus, long-range AF order may occur even in spin-gapped compounds, likely as it happens in the Zn-doped two-leg $s = 1/2$ -ladder SrCu_2O_3 [12, 13]. Theory also predicts that owing to the coupling of the impurity induced spin states with the host spin lattice the former may interact strongly via the AF background [14]. Experimentally one finds, that, for instance, Zn-doping induced spin moments in the CuO_2 planes of $\text{La}_{1-x}\text{Sr}_x\text{CuO}_4$ indeed order antiferromagnetically below the Néel temperature of the Cu spin lattice [15]. Recently, experimental indication of the strong interaction between impurity and bulk spins in the $s = 1/2$ low-D HAF CaCu_2O_3 have been reported by Kiryukhin *et al.* [16]. CaCu_2O_3 has a crystal structure similar to the two-leg spin-ladder compound SrCu_2O_3 which exhibits a large spin gap of about 420 K and is nonmagnetic at low T [17]. However, in contrast to the Sr counterpart where Cu spin chains parallel to the b axis are coupled in the ab planes into ladders via a strong rung AF exchange, in CaCu_2O_3 the Cu-O-Cu bond angle in the rungs deviates significantly from 180° , resulting in a reduced rung coupling (figure 1). Remarkably, no hint for a spin gap in the Ca compound was obtained so far. This suggests that the corrugation of the ladders changes the spin topology from nearly isolated two-leg ladders to pseudo-ladders with significant interladder interactions, i.e. the coupled spin chains in this pseudo-ladder compound form anisotropic bilayers parallel to the bc plane [16, 18, 19, 20]. Owing to an appreciable inter-plane magnetic exchange along the c direction J_c concomitant with a strongly reduced rung interaction J_r CaCu_2O_3 orders antiferromagnetically at $T_N \simeq 25$ K [16, 21]. Below 300 K the magnetic susceptibility χ of CaCu_2O_3 is quite small due to the strong intra-chain AF coupling $J_b = J_{\parallel} \sim 2000$ K. The observed weak Curie-like T dependence of $\chi(T < 300 \text{ K})$ suggests that the magnetization in this temperature range is determined by a small amount of uncompensated spins. Surprisingly, a strong reduction of the susceptibility χ below T_N suggests that these spin states participate in the AF ordering of the host and therefore cannot be ascribed to some impurity phase [16].

To get more insight into the unusual interplay between the "extra" spins and the host spin lattice, we have measured electron spin resonance (ESR) of single crystals

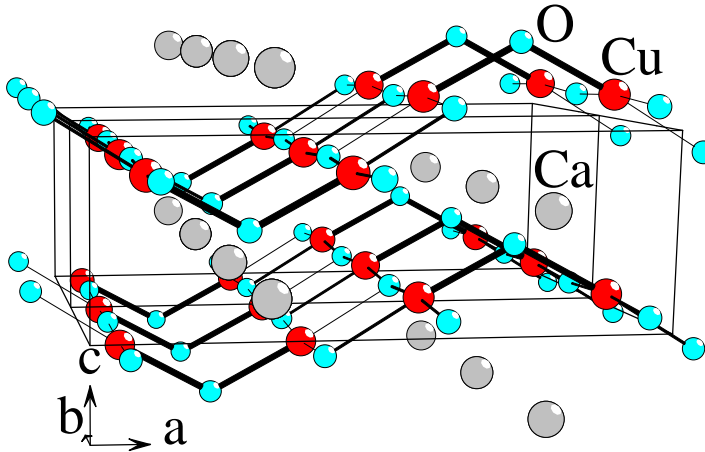


Figure 1. The crystal structure of CaCu_2O_3 . Cu-O chains running along the b axis are coupled into two-leg ladders. Strongly bent rung bonds in the ladders are visualized by thick lines.

of CaCu_2O_3 in the sub-Terahertz frequency range in pulsed magnetic fields. ESR measurements which probe locally the magnetism of paramagnetic centres show clearly that in fact these spins are involved in the magnetic ordering. The interplay with the host shows up in the critical broadening of the spectrum at $T \gtrsim T_N$, as well as in the reduction of the intensity of the signal and the shift of the resonance field at $T < T_N$. Remarkably, in fields above 20 T these features are not present anymore: The ESR signal narrows and its intensity increases down to the lowest temperature indicating the reduction of the AF fluctuations and of the long-range order. The field dependence of the ESR line reveals a small gap of the order of $\sim 0.3 - 0.8$ meV for magnon excitations in the ordered state which can explain the occurrence of a spin-flop transition at a relatively small magnetic field of ~ 3 T. Our ESR data suggest that such "extra" states may interact strongly with the host spin lattice in CaCu_2O_3 which may be also of relevance for the magnetic ordering of the other frustrated low-dimensional quantum antiferromagnets.

2. Experiment and results

CaCu_2O_3 crystallizes in the orthorhombic symmetry, space group Pmmn , with $a = 9.949$ Å, $b = 4.078$ Å and $c = 3.460$ Å at $T = 10$ K. Single crystals studied in the present work have been grown using the travelling solvent floating zone (TSFZ) method with CuO as a flux. The details of the sample preparation and their characterization can be found in Ref. [16]. The electron probe microanalysis data taken at 10 points of the crystal surface of size 2×2 mm² reveal the following composition of the elements. Ca: 0.854 (0.023), Cu: 2.039 (0.056) and O: 3.005 (0.082). We note that an appreciable excess of Cu and a respective deficiency of Ca is quite typical for this material [21].

The high field ESR experiments were performed up to 40 T in a resistive coil driven

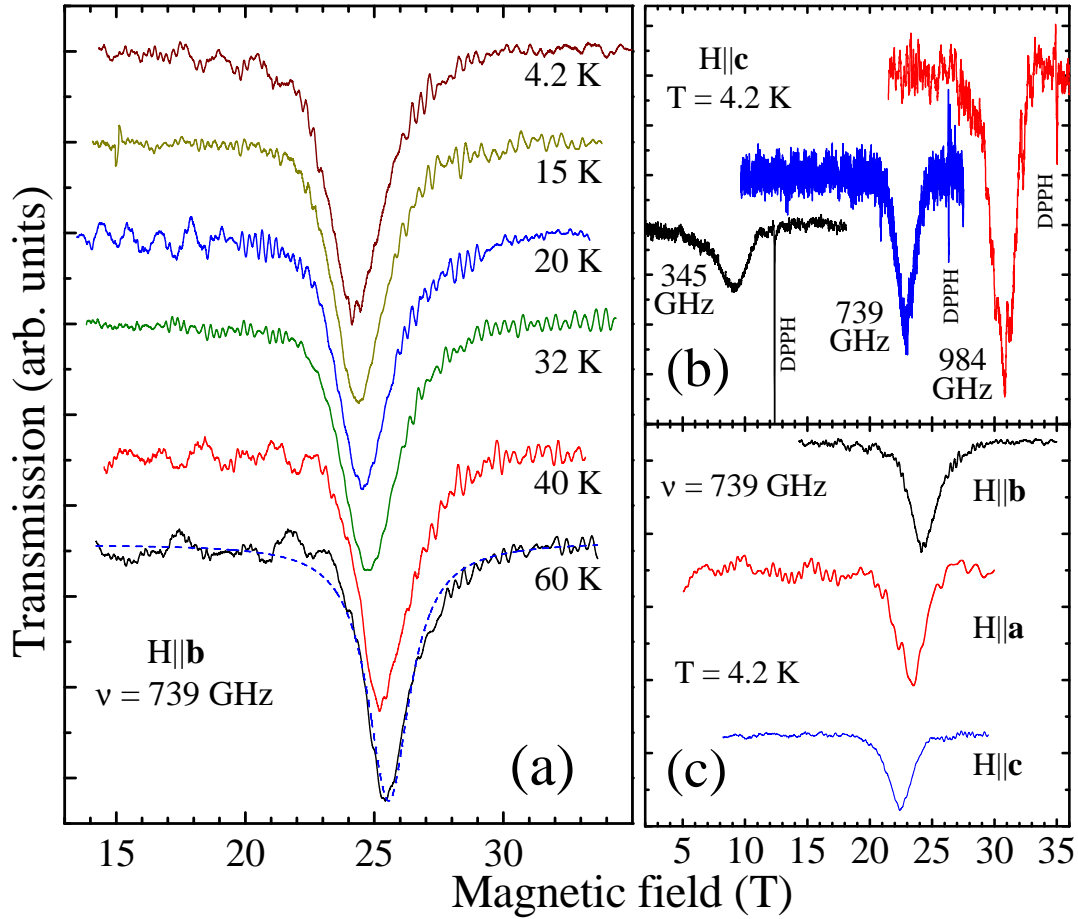


Figure 2. Representative ESR spectra of CaCu_2O_3 : (a) ESR signal at 739 GHz for $H \parallel b$ axis at several selected temperatures. The dashed curve is a representative Lorentzian fit of the signal at $T = 60$ K; (b) The ESR signal at different frequencies for $H \parallel c$ axis at 4.2 K. Sharp resonances correspond to the diphenyl-picryl-hydrazyl (DPPH) field marker; (c) ESR spectra at 739 GHz and 4.2 K for H applied along three crystallographic axes a , b and c , respectively.

by a capacitor bank. The three principal axes of the single crystal were successively set parallel to the magnetic field. The excitation energies were provided by an optically pumped far infrared cavity and by a Gunn diode (96 GHz). Conventional ESR measurements in the X-band were performed with a Bruker ESP 300 E Spectrometer. Magnetic susceptibility in the temperature range 2 K - 300 K and magnetization measurements up to 5 T were carried out with a Quantum Design Superconducting Quantum Interference Device. Conventional ESR measurements at a frequency $\nu \simeq 10$ GHz (X-Band) yield no signal and those at $\nu \simeq 100$ GHz reveal only a very weak resonance response which cannot be associated with strong changes of bulk magnetic properties at low temperatures. In contrast, an order of magnitude stronger resonance absorption has been observed at much higher frequencies and much stronger magnetic fields. Representative ESR spectra of CaCu_2O_3 in the sub-Terahertz frequency domain are shown in figure 2. The ESR spectrum consists of a single line close to a Lorentzian

shape with a slightly anisotropic resonance field H_{res} typical for the resonance response of the Cu^{2+} ions with anisotropic g factor (see below). By fitting the signal with a Lorentzian line profile the intensity I , the resonance field H_{res} and the width ΔH of the resonance have been determined. The temperature dependence of these quantities is shown in figure 3 for the case of $H \parallel c$ axis.

In pulsed magnetic field experiments the accurate determination of the intensity of the ESR line is difficult due to the poor signal-to-noise ratio as compared to conventional ESR technique. Moreover, a large background due to the voltage induced in the detector by the field pulse has to be subtracted from the total signal. Therefore the data shown in figure 3(a) have large error bars and scatter considerably. Owing to these technical problems the ESR intensities I obtained at different frequencies cannot be directly compared and the $I(T)$ dependences in figure 3(a) at each frequency are normalized to a respective 4.2 K value. Fortunately, the linewidth ΔH and the resonance field H_{res} can be measured with a much better accuracy. One can recognize noticeable differences in the behaviour of these parameters vs. temperature, depending on the excitation frequency and thus on the field range of the measurement. ΔH increases at the smallest ESR frequency $\nu = 344$ GHz appreciably in the temperature range $25 \text{ K} \lesssim T \lesssim 60 \text{ K}$ and saturates below 25 K. (figure 3(b)). However, the ESR signal measured at higher frequencies and much stronger magnetic fields shows a continuous decrease of ΔH in the whole temperature range. H_{res} is practically constant at higher temperatures and decreases below ~ 25 K, as can be seen in figure 3(c). Note that the shift of the resonance is most pronounced for the smallest ESR frequency and the field of the measurement. This is illustrated in figure 4 where the shift of H_{res} at $T = 4.2$ K relative to its high temperature value is plotted as a function of magnetic field H .

Remarkable changes of ESR at low T are evident also in figure 5 where the ν vs. H_{res} diagram at a high (80 K) and at a low temperature of 4.2 K is shown in the inset and in the main panel, respectively. It is possible to fit these data assuming a simple linear frequency/field relation in a form $\nu = \Delta + (g\mu_B/h)H$, where Δ is the zero-field frequency offset, g is the Lande g factor, μ_B is the Bohr magneton and h is the Planck constant, respectively. The fit at $T = 80$ K yields g factors amounting to 2.21 and 2.08 for $H \parallel c$ and b axes, respectively, which is usual for a Cu^{2+} ion in a square-planar ligand coordination (figure 1). The offset Δ is negligibly small, as expected for ESR of a $S = 1/2$ paramagnetic ion having a Kramers degeneracy of the ground state. In contrast, the fit at $T = 4.2$ K yields an appreciable offset $\Delta \simeq 70$ GHz corresponding to about 0.3 meV, or 3.4 K, which signals the occurrence of an energy (magnon) gap at low temperatures.

3. Discussion

Obviously, considerable changes of ESR in the low-temperature regime are related to the AF order of CaCu_2O_3 . The T dependence of the static magnetic susceptibility $\chi(T)$ and the field dependence of the magnetization $M(H)$ at $T = 4.2$ K of the studied

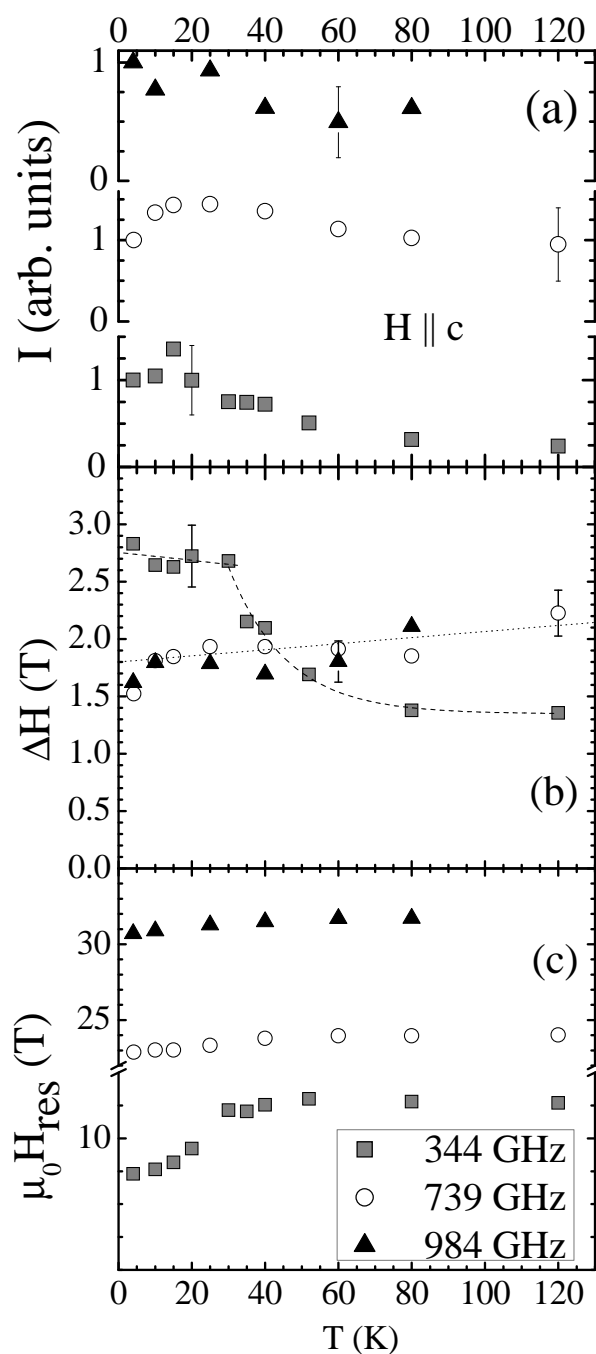


Figure 3. Temperature dependence of the intensity $I(T)$ normalized to the value at 4.2 K (a), the width $\Delta H(T)$ (b) and the resonance field $H_{res}(T)$ (c) of the ESR signal measured at frequencies 344 GHz, 739 GHz and 984 GHz, respectively, for the direction of the magnetic field parallel to the c axis. Dotted and dashed lines are guides for the eye. The error bars in (c) are within the size of the symbols.

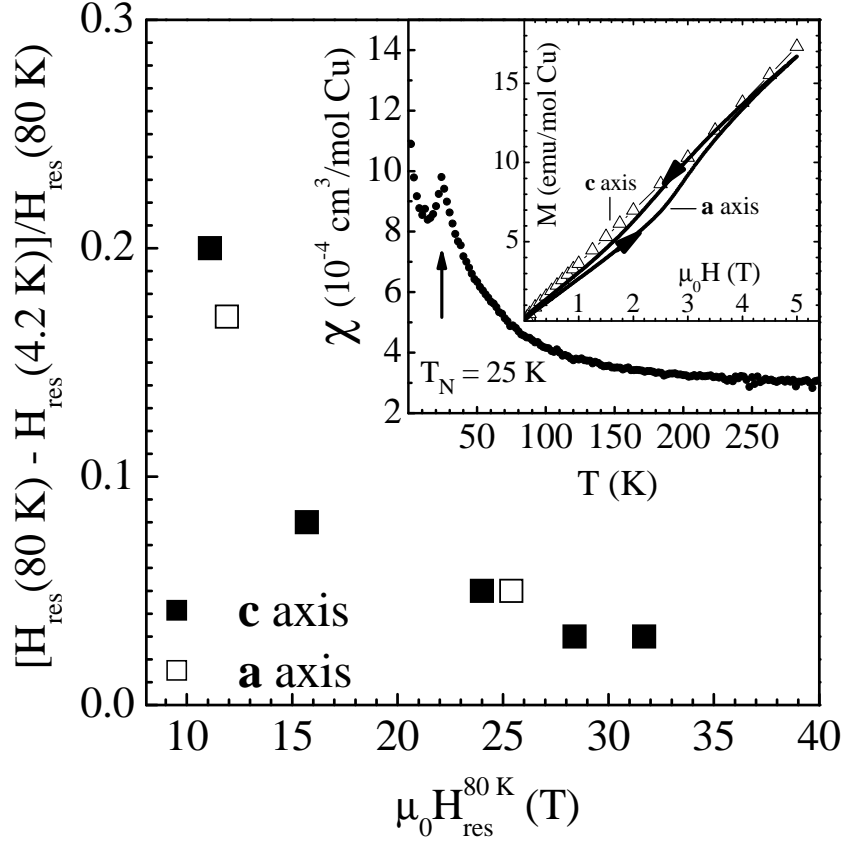


Figure 4. The relative shift of the resonance field H_{res} at $T = 4.2$ K as a function of the magnetic field. Inset: Temperature dependence of the static magnetic susceptibility $\chi(T)$ measured at $H = 25$ Oe for $H \parallel a$ axis, and the field dependence of the magnetization $M(H)$ for $H \parallel a$ and c axes at $T = 4.2$ K. Note the Néel peak in $\chi(T)$ indicating a transition to the AF ordered state at $T_N = 25$ K and a nonlinear hysteresis behaviour of $M(H)$ for $H \parallel a$ evidencing a field-induced spin-flop transition at $\mu_0 H_{sf} \sim 3$ T.

crystal are shown in the inset of figure 4. Consistently with the results of Kiryukhin *et al.* [16] the $\chi(T)$ dependence reveals a characteristic Néel peak at $T_N = 25$ K signalling an AF phase transition, whereas a nonlinear behaviour of $M(H)$ for $H \parallel a$ axis can be attributed to a spin-flop transition at $\mu_0 H_{sf} \sim 3$ T [16]. In fact, the condition for the occurrence of the magnetic ground state in coupled spin chains derived recently by Sengupta *et al.* [20], $J_r/J_b \leq 2.53\sqrt{J_c/J_b}$, which relates the strength of the intra-chain exchange $J_b \sim 2000$ K, the inter-plane exchange $J_c \sim 100$ K and the exchange coupling in the rungs $J_r \sim J_c$ [19, 16], respectively, is easily satisfied in CaCu_2O_3 using the estimate $J_b/J_c \sim 20$ obtained from the experimentally observed magnetic moment $\mu = 0.2\mu_B$ [19, 16]. Remarkably, the onset of the decrease of H_{res} as well as the kink in the dependence $\Delta H(T)$ at $\nu = 344$ GHz coincides with the AF phase transition at 25 K. Observation of the frequency offset Δ gives evidence for the opening of the gap for magnon excitations below T_N . In fact, the simple linear interpolation of the data points in figure 5 sets the smallest possible gap because the

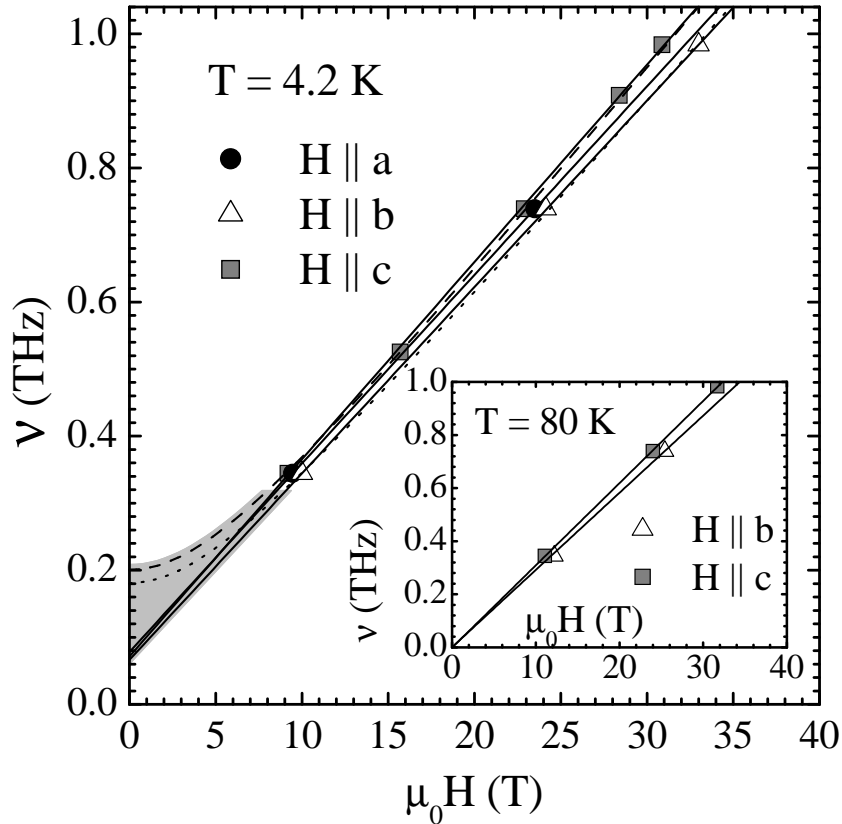


Figure 5. Frequency ν vs. resonance field H_{res} diagram for different directions of the magnetic field at 4.2 K (main panel) and 80 K (inset), respectively. The solid lines are linear fits to the experimental data. The dashed and dotted lines represent a square root dependence $\nu = \sqrt{\Delta^2 + (g\mu_B/h)^2 H^2}$. The shaded area indicates an uncertainty in the determination of the gap. (See the text)

$\nu(H)$ dependence may saturate at low fields. E.g. in a simple case of a collinear "easy axis" or an "easy plane" antiferromagnet one expects for the "hard" direction a square root dependence of ν on H in a form $\nu \simeq \sqrt{\Delta^2 + (g\mu_B/h)^2 H^2}$ [22]. Applying this relation to experimental data yields a larger value of the gap $\Delta \simeq 200$ GHz (figure 5) corresponding to 0.8 meV, or 10 K. From our data it is not possible to discriminate between these two behaviours which brings an uncertainty in the determination of the gap indicated by a shadowed area in figure 5. The assignment of the small spin gap to the host or to the minority spin subsystem is difficult at present, since the coupled subsystems may exhibit rather different gaps in each subsystem despite the identical critical temperature. In the absence of the long-range order a small spin gap may arise if spin chains are cut by structural imperfections in segments of a finite length. In this scenario "extra" spin states in a concentration x may reside at the spin chain boundaries and one would expect the corresponding impurity induced finite size gap of the order of $\Delta_L = 0.5\pi^2 x J_b \sim x 10^4$ [K] [23]. Such a singlet/triplet gap can be directly observed in ESR [24] in the presence of the alternating g tensor and the anisotropic

Dzyaloshinsky-Moriya (DM) interaction [25]. However, taking the values of the intra-chain AF coupling $J_b \sim 2000$ K and the gap $\Delta = 3.4 - 10$ K one would arrive at an extremely low concentration of defects $x = \Delta_L/0.5\pi^2 J_b \lesssim 10^{-3}$ whereas the static susceptibility data yield much larger value of x in the range of a few percent. In this case a gap of the order of 100 K should be expected but which is not observed. Hence, a simple interruption of chains as the cause of the observed spin gap in CaCu_2O_3 is unlikely. This suggests that the defect related minority spins should reside outside the zigzag chains/pseudo-ladders [26]. Such an appropriate position would be given e.g. by some Cu^{2+} ions substituted for Ca.

Indeed, in a detailed structure analysis by Ruck *et al.* [21] a sizeable amount of excess Cu $\sim 10\%$ (up to 14%) and some oxygen O(2) deficiency on a pseudo-ladder rung of about 2 % has been found by analyzing electron density measurements (Fourier synthesis with x-ray data). Similar appreciable deviations from the stoichiometry are found in our crystals too (see Section 2). Using the simple concept of bond length considerations for the Cu valency ν_{Cu} versus bond lengths $s_{\text{Cu-O}}$ by Brown, Altermatt and O' Keeffe [32]

$$\nu_{\text{Cu}} = \sum s_{\text{Cu-O}} = \sum \exp[(r_0 - r)/B], \quad (1)$$

where $B = 0.37 \text{ \AA}$ is an empirical factor, $r_0(\text{Cu}^{2+})=1.679 \text{ \AA}$ and $r_0(\text{Cu}^{1+})=1.593 \text{ \AA}$ are the ionic radii of Cu in a 2+ and 1+ oxidation states, respectively, Ruck *et al.* [21] ascribed the excess Cu solely to nonmagnetic Cu^{1+} residing close to a Ca position. However, near an O(2) vacancy such a position becomes unstable since the Cu-ion is now attracted by the two O(2)-ions belonging to a regular, i.e. oxygen non-deficient, rung of an adjacent pseudo-ladder. As a result the corresponding small part of those Cu ions near an O(2) vacancy is likely to be shifted towards that nearest regular rung, i.e. they will occupy real interstitial positions. This situation is illustrated in figure 6, where in the left panel the formal valency of a Cu ion in dependence on its position along the c axis between two neighbouring rungs according to Eq. (1) is depicted. In fact, a self-consistent Cu^{2+} position occurs about 1.5 \AA above the regular rung, i.e. *inside* a buckled pseudo-ladder far from the self-consistent Cu^{1+} position about 0.55 \AA below the opposite regular rung *outside* a buckled pseudo-ladder. The different positions of these "defect" Cu^{1+} and Cu^{2+} sites with respect to the ladders are sketched in the right panel of figure 6. In particular, the position of the off-ladder Cu^{2+} ion allows for a coupling J_{eh} of its spin with the Cu spins at the regular lattice sites to the left and to the right, respectively, along the a axis (see below). We note that such a small amount of "defect" Cu^{2+} ions is in agreement with the small number of "extra" spins as deduced from the magnetic susceptibility measurements.

Anyhow, the occurrence of a magnon gap in an AF ordered $s = 1/2$ magnet is usually related with additional anisotropic corrections to the main isotropic Heisenberg exchange. In case of CaCu_2O_3 it may be the DM interaction [25] which is, in principle, allowed in this compound owing to the missing inversion symmetry centre between the neighbouring Cu ions (figure 1). Moreover, the assumption of the DM interaction

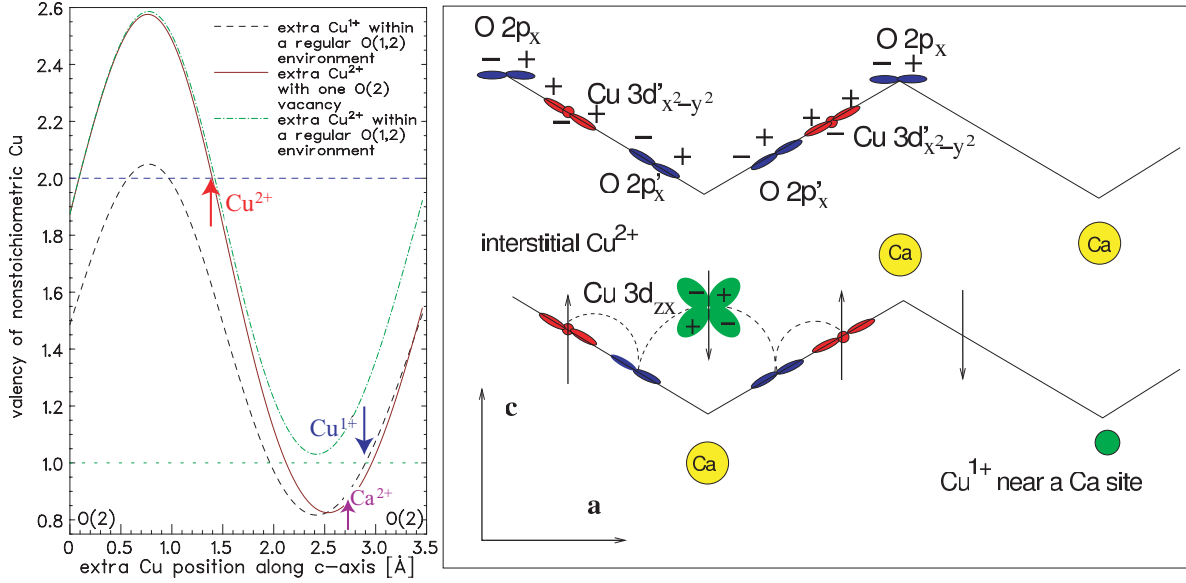


Figure 6. Left panel: Cu valency vs. position along the c axis in between two adjacent rung centres according to Eq. (1). Equilibrium positions of the "defect" Cu^{1+} and Cu^{2+} sites as well as of the Ca^{2+} regular site are indicated in the plot adopting r_0 for Cu^{1+} and Cu^{2+} , respectively, (see Eq. (1)). Right panel: The main orbitals involved in the exchange interaction between an interstitial Cu^{2+} ion and the regular Cu^{2+} ions in the buckled pseudo-ladder structure of CaCu_2O_3 . The notation of orbitals with a prime corresponds to the local system of coordinates adopted to the zigzag (double) CuO_2 chains rotated alternately around the b axis. The signs \pm stand for the phases of the p and d orbitals. The Cu^{1+} ion positions are shifted closer to the buckled rung lines as compared to the Ca position (cf. left panel). Note the downshift of the interstitial Cu^{2+} ion which facilitates the coupling of its spin with the Cu spins at the regular pseudo-ladder sites. The relevant superexchange paths are indicated by dashed lines.

between the spins in the ladder rung naturally explains details of the the incommensurate spin structure in CaCu_2O_3 [16]. In fact, the observed noncollinearity of the rung magnetic moments defined by the angle η (see figure 7) as well as the related deviation from the antiferromagnetic orientation, measured by the angle $\Theta_r = \pi - \eta$, is directly connected to the presence of DM interactions $\mathbf{D} \parallel \mathbf{b}$. In classical spin and nearest neighbour approximations it simply reads $\tan \Theta_r = D/J_r \approx 0.4$, where the experimental value $\eta \approx 160^\circ$, from the neutron scattering data [16], has been used. Adopting $J_r \sim 10$ meV [16, 19] a sizeable DM exchange $D \sim 4$ meV would be expected. Comparing this value with that for the well-known 2D cuprate La_2CuO_4 of 5 meV [33] or of about 1.5 meV for the edge-shared chain compound Li_2CuO_2 [34] i.e. all values being significantly larger than the gap derived from the ESR data, one might conclude that in our case the spin gap could be ascribed to the coupling between the minority and majority spin subsystems. (We note that the single-ion anisotropy is absent in the $S = 1/2$ case.) Indeed the position of a Cu^{2+} ion at a low-symmetry interstitial site allows also the occurrence of DM interaction terms for the "extra" spin-host exchange in addition to the isotropic symmetric exchange J_{eh} shown in figure 7 (see below). The small value

of the spin gap found in the present work is in agreement with recent inelastic neutron scattering data [35]. No gap exceeding the experimental resolution limit of 3 meV has been found, which sets an upper bound for a possible spin gap in CaCu_2O_3 . The possible upper bound can be further reduced to ~ 0.8 meV based on our ESR analysis (figure 5). Moreover it yields also a lower bound of about 0.3 meV.

The magnitude of the anisotropy gap in CaCu_2O_3 amounting to less than 10 K sets the respective field scale of a few Tesla for the spin-flop transition $H_{sf} = \Delta/g\mu_B$ [22], which indeed occurs at $\mu_0 H_{sf} \sim 3$ T (see figure 4 and Ref. [16]). At fields $H > H_{sf}$ one expects a reduction of the staggered field and saturation of the uniform spin susceptibility χ_s below T_N . This effect is particularly appreciable in strong magnetic fields yielding the decrease of the resonance shift (Figs. 3c and 4). Furthermore, the T dependence of the resonance linewidth $\Delta H(T)$ measured at 23 and 32 T changes qualitatively as compared to ESR in the "small" field of 11 T giving a hint for possible recovery of the paramagnetic state in strong fields. In low-dimensional spin systems the slowing down of the short-range AF fluctuations sets in at temperatures far above T_N which results in a continuous growth of the ESR width by approaching T_N [36]. This kind of behaviour is seen in the $\Delta H(T)$ dependence at the lowest resonance field of ~ 11 T (figure 3b). However, at stronger magnetic fields of 24 and 32 T the signal *narrows* continuously in the whole temperature range giving evidence for a strong suppression of AF correlations in CaCu_2O_3 by magnetic field. Theoretical calculations [37] show that in a low-dimensional antiferromagnet the ESR critical broadening scales with the spin-correlation length ξ which implies that in CaCu_2O_3 ξ reduces significantly in strong magnetic fields. These ESR findings corroborate the results of elastic neutron scattering in Ref. [16] which yield a finite ξ of the order of 250 Å already in a moderate magnetic field of 8 T indicating the loss of the long-range AF order.

A strong sensitivity of the magnetic order in CaCu_2O_3 to magnetic field is quite surprising because the magnetic energy scale is much smaller than the leading exchange couplings in the system. One may speculate that owing to the frustration of the magnetic exchange [18, 19] the minority spin subsystem plays a decisive role for the stabilization of the long-range Néel state. In particular, if the "extra" spins reside at interstitial positions, as discussed above, they are likely to mediate the second neighbour inter-ladder interaction in the highly frustrated a direction (figure 6 and 7). This antiferromagnetic coupling J_{eh} is responsible for the intermediate commensurate neutron scattering magnetic h peaks shown in Figs. 6 and 8 of Ref. [16] and helpful to promote the 3D AF order. It arises from a similar superexchange process as that which creates the leading coupling along the legs $J_l \sim 2000$ K but it is strongly reduced by the buckling and by the out-off-pseudo-ladder position of the "extra" (interstitial) Cu^{2+} site (figure 6). Applying standard 4th order perturbation theory within a pd -multiband extended Hubbard model (see e.g. Ref. [38]) and the angular dependences for the Slater-Koster integrals from Refs. [39, 40], we may estimate $J_{eh} \approx \sin^2(\Theta') \sin^2(0.5(\Theta_r - \Theta')) f J_l \sim 8 - 30$ K, where Θ_r and Θ' denote the buckling angle and the O(1) - "extra" Cu^{2+} site - O(1) angle, respectively (see above). Here $f \lesssim 1$

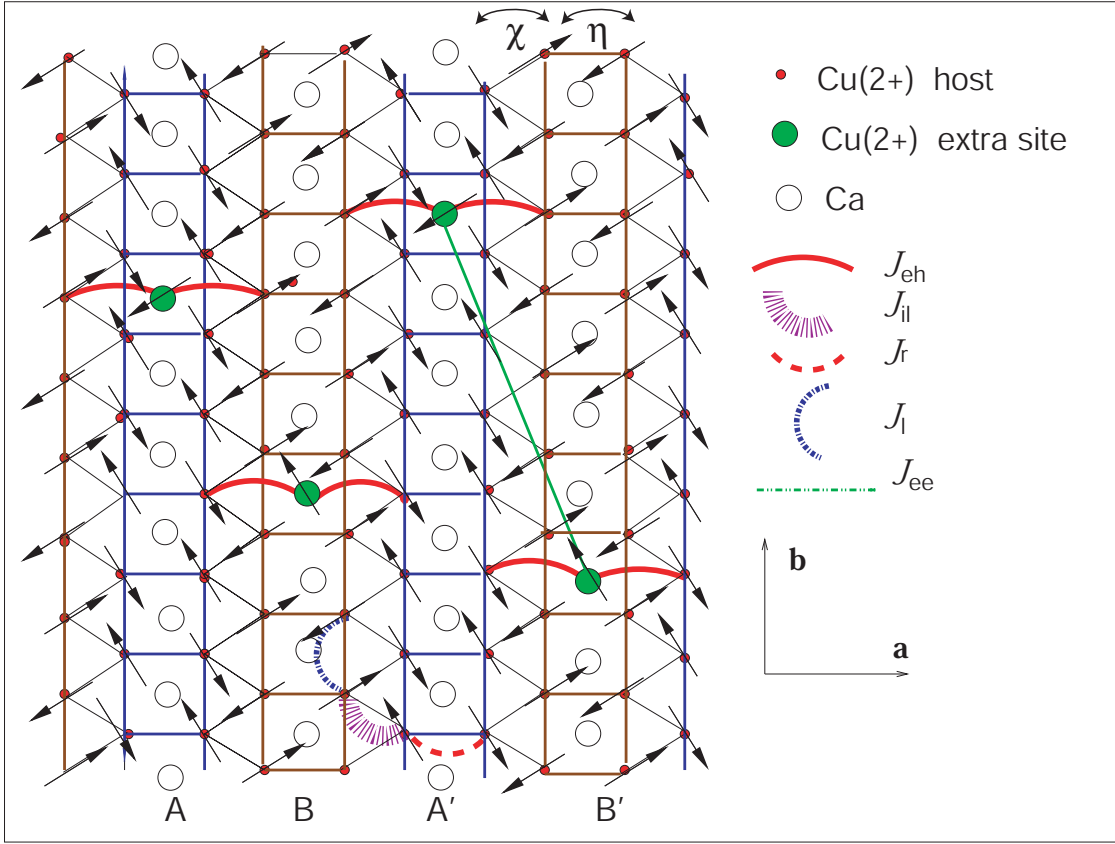


Figure 7. Schematic magnetic structure of a buckled plane of pseudo-ladders in CaCu_2O_3 projected on the (ab) plane with the most important exchange interactions according to Eq. (2). Intra-ladder exchange along the legs and rungs, J_l and J_r , is sketched by red-dashed and blue arcs, respectively. Frustrated inter-ladder exchange J_{il} is shown by magenta arc. Much weaker exchange paths connecting "extra" spins at the Cu^{2+} out-off ladder positions with the regular spin lattice and the coupling between the "extra" spins are depicted by solid red arcs and a green dash-dotted line, respectively. η and χ designate the angles between adjacent spins on the rungs and between the two legs of neighboring ladders, respectively. Note, that in the real structure these angles slightly deviate from the ideal values of π and $\pi/2$, cf. Fig. 1 of Ref. [16]. (see the text for details)

is a further reduction factor due to the larger distance between O(1) and the mentioned off ladder position of the "extra" spins compared with the usual Cu-O distance of about 1.9 \AA in planar CuO_4 plaquettes. Here a Cu $3d_{zx}$ or a mixed $3d_{zx}-3d_{yz}$ state for the "extra" spins has been adopted (figure 6). Noteworthy, the estimated above "extra" spin-host spin exchange J_{eh} is of the same order as the ordering temperature T_N suggesting that indeed the "extra" spin states are relevant for the long-range AF order and might also help developing the incommensurate spin structure. Remarkably, the weak commensurate correlation has been observed in the neutron-diffraction scans up to the highest applied field of 8 T whereas the incommensurate one is shifted and/or suppressed (see figure 8 of Ref. [16]). Owing to a small concentration of "extra" spins

the coupling between them, most probably of the dipolar character, is expected to be very small $J_{ee} < 1 \text{ mK}$ and can be neglected. Thus, we arrive finally at an hierarchy of exchange integrals:

$$J_l > J_r \sim |J_{il}| \gg J_{eh} \gg |J_{ee}|, \quad (2)$$

where J_{il} denotes the ferromagnetic interladder exchange which is of the order of the rung exchange J_r . As the last two exchange integrals in Eq. (2), J_{eh} and J_{ee} , are relatively weak and from the remaining frustration in the nearest neighbour inter-ladder coupling, one indeed may expect a strong influence already of a moderate field on the magnetic order. The relevant interaction paths yielding the spin structure of CaCu_2O_3 are shown in figure 7. The drawn spin lattice has been simplified for clarity: (i) To emphasize that the observed commensurate component in the elastic structure factor (Ref. [16]) is caused by the AF "extra" spin - host spin interaction J_{eh} a slight incommensurability along the a axis ([0.429,0.5,0.5]) due to the frustrating inter-ladder exchange J_{il} within local triangles of the Cu host spins has been ignored; (ii) In the real structure both the depicted antiparallel spin arrangement on the rungs and the orthogonal orientation at the inter-ladder borders are slightly distorted; (iii) Due to the presence of DM interactions for neighbouring spins at the buckled rungs, the magnetic moments are not in the (ab) plane, but within the (ac) plane. (iv) The pseudo-ladders A(A') and B(B'), respectively, being relatively shifted by $0.5b$ along the b axis are alternatingly buckled (cf. figure 1).

Because of the relative smallness of the "extra" spin - host spin exchange J_{eh} as compared to other exchange integrals the relaxation of "extra" spins can be treated in a close analogy to nuclear magnetic resonance where the nuclear spin relaxation rate $1/T_1$ is determined by a fluctuating hyperfine field of electron spins [41]. Following this analogy the T_1 -contribution to the ESR linewidth of "extra" spins $\Delta H \sim 1/\gamma T_1$ is given by the dynamical susceptibility $\chi(\omega)$ of the host spins $1/T_1 T \sim J_{eh} \text{Im}(\chi(\omega))/\omega$ [42, 43]. Here γ is the gyromagnetic ratio. Since the AF correlation length ξ is inversely related to the frequency of the fluctuations of the spins, the increase of ξ will result in the slowing down of spin fluctuations, i.e. to the shift of the spectral weight of the dynamical susceptibility of bulk spins to lower frequencies, comparable with the ESR excitation frequency, and consequently to a strong broadening of the ESR signal of "extra" spins. Thus the suppression of the long-range AF order and spin fluctuations by a strong magnetic field may explain why the ESR signal is observable only at sub-Terahertz frequencies and not in the low-frequency domain of 10 – 100 GHz. Plausibly the corresponding resonance field of at most 3 T is not sufficient to suppress AF fluctuations which broaden the resonance line very strongly. Even at a much higher frequency of 344 GHz the width of the ESR signal approaches 3 T at low T . The detection of such a broad resonance at smaller probing frequencies would be hardly possible [44].

4. Conclusions

We have measured high field ESR of a small amount of "quasi-free" spins which determine the bulk static magnetic properties of a $s = 1/2$ -pseudo-ladder compound CaCu_2O_3 at low temperatures. The frequency-, magnetic field- and temperature dependences of the ESR signal show that these "extra" spin states are strongly coupled to the bulk spins and are involved in the AF ordering of the host spin lattice at $T_N = 25$ K. In particular, ESR gives evidence for the opening of a gap for magnetic excitations below T_N whose small magnitude explains the occurrence of a spin-flop transition in a small magnetic field of ~ 3 T. Another remarkable observation is the narrowing of the ESR line at fields above 20 T which signals the suppression of AF correlations and may indicate the loss of the long-range magnetic order in strong magnetic fields. Experimental ESR data corroborate theoretical predictions of a strong interplay between "extra" spin states at the imperfections of the host AF $s = 1/2$ -lattice with the bulk spins.

Acknowledgement

The DFG under project SP 1073 (S-LD and BB) is gratefully acknowledged for financial support. Work of RK in Toulouse was supported by the DFG through KL 1824/1-1. This work was also supported in part by the MRSEC Program of the National Science Foundation under award number DMR 02-13282. We thank C Hess, B Lake, G Krabbes, A Moskvina, K-H Müller and M Wolf for useful discussions.

References

- [1] Mikeska H J and Kolezhuk A K in *Quantum magnetism* ed U Schollwöck *et al.* (Berlin: Springer) 2004 *Lecture Notes in Phys.* **645**
- [2] Xiao G, Cieplak M Z, Xiao J Q and Chien C L 1990 *Phys. Rev. B* **42** R8752
- [3] Finkelstein A M, Kataev V E, Kukovitskii E F and Teitelbaum G B 1990 *Physica C* **168** 370
- [4] Alloul H, Mendels P, Casalta H, Marucco J F and Arabski J 1991 *Phys. Rev. Lett.* **67** 3140
- [5] Khaliullin G, Kilian R, Krivenko S and Fulde P 1997 *Phys. Rev. B* **56** 11882
- [6] Vojta M, Buragohain C and Sachdev S 2000 *Phys. Rev. B* **61** 15152
- [7] Wang Z and Lee P A 2002 *Phys. Rev. Lett.* **89** 217002
- [8] Höglund K H and Sandvik A W 2003 *Phys. Rev. Lett.* **91** 077204
- [9] Bulut N, Hone D, Scalapino D J and Loh E Y 1989 *Phys. Rev. Lett.* **62** 2192
- [10] Martins G B, Laukamp M, Riera J and Dagotto E 1997 *Phys. Rev. Lett.* **78** 3563
- [11] Laukamp M, Martins G B, Gazza C, Malvezzi A L, Dagotto E, Hansen P M, López A C and Riera J 1998 *Phys. Rev. B* **57** 10755
- [12] Azuma M, Fujishiro Y, Takano M, Nohara M and Takagi H 1997 *Phys. Rev. B* **55** R8658
- [13] Ohsugi S, Tokunaga Y, Ishida K, Kitaoka Y, Azuma M, Fujishiro Y and Takano M 1999 *Phys. Rev. B* **60** 4181 (1999); Fujiwara N, Saito T, Azuma M and Takano M 2000 *Phys. Rev. B* **61** 12196
- [14] Chen Y C and Castro Neto A H 2000 *Phys. Rev. B* **61** R3772
- [15] Hücker M and Büchner B 2002 *Phys. Rev. B* **65** 214408

- [16] Kiryukhin V, Kim Y J, Thomas K J, Chou F C, Erwin R W, Huang Q, Kastner M A and Birgeneau R J 2001 *Phys. Rev. B* **63** 144418
- [17] Azuma M, Hiroi Z, Takano M, Ishida K and Kitaoka Y 1994 *Phys. Rev. Lett.* **73** 3463
- [18] Kim T K, Rosner H, Drechsler S-L, Hu Z, Sekar C, Krabbes G, Málek J, Knupfer M, Fink J and Eschrig H 2003 *Phys. Rev. B* **67** 024516
- [19] Drechsler S-L, Rosner H, Kim T K, Knupfer M, Eschrig H and Málek J 2004 *Physica C* **408-410** 270
- [20] Sengupta P, Zheng W and Singh R R P 2004 *Phys. Rev. B* **69** 064428
- [21] Ruck K, Wolf M, Ruck M, Eckert D, Krabbes G and Müller K-H 2001 *Mat. Res. Bull.* **36** 2001
- [22] Turov E A 1965 *Physical Properties of Magnetically Ordered Crystals* (New York: Academic Press)
- [23] Asakawa H, Matsuda M, Minami K, Yamazaki H and Katsumata K 1998 *Phys. Rev. B* **57** 8285
- [24] Sakai T, Cépas O and Ziman T 2000 *J. Phys. Soc. Japan* **69** 3521
- [25] Dzyaloshinsky I 1958 *Phys. Chem. Solids* **4** 241; Moriya T 1960 *Phys. Rev.* **120** 91
- [26] The estimate of the density of impurity spins is in accord with estimates of the magnetic mean-free path l_{mag} from magnetic thermal transport, Hess C, ElHaes H, Waske A, Sekar C, Krabbes G, Büchner B., Heidrich-Meisner F and Brenig W, to be published.
The thermal conductivity tensor κ of CaCu_2O_3 is found to be highly anisotropic with $\kappa_b \gg \kappa_a, \kappa_c$, where κ_b strongly increases with temperature, while κ_a, κ_c are only weakly temperature dependent. Similar evidence for magnetic heat transport has been reported for closely related quasi one-dimensional quantum magnets such as $(\text{Sr,Ca,La})_{14}\text{Cu}_{24}\text{O}_{41}$ [27, 28, 29], SrCuO_2 and Sr_2CuO_3 [30]. The calculation of l_{mag} in CaCu_2O_3 has been done in the framework of kinetic transport theory in analogy to the procedure described in [28]. The result yields $l_{mag} \approx 25 \text{ \AA}$. Assuming that this value gives the length-scale for the mean distance between defects [31], in our model this would correspond to the density of defects of about $\sim 8\%$.
- [27] Sologubenko A V, Gianno K, Ott H R, Ammerahl U and Revcolevschi A 2000 *Phys. Rev. Lett.* **84** 2714
- [28] Hess C, Baumann C, Ammerahl U, Büchner B, Heidrich-Meisner F, Brenig W and Revcolevschi A 2001 *Phys. Rev. B* **64** 184305
- [29] Hess C, ElHaes H, Büchner B, Ammerahl U, Hücker M and Revcolevschi A 2004 *Phys. Rev. Lett.* **93** 027005
- [30] Sologubenko A V, Gianno K, Ott H R, Vietkine A Revcolevschi A 2001 *Phys. Rev. B* **64** 054412
- [31] Hess C, Ribeiro P, Büchner B, ElHaes H, Roth G, Ammerahl U and Revcolevschi A 2006 *Phys. Rev. B* **73** 104407
- [32] Brown I D and Altermatt D 1985 *Acta Crystallogr. B* **41** 244; Breese N E and O’Keeffe M 1991 *ibid.* **47** 192
- [33] Keimer B, Birgenau R J, Cassanho A, Endoh Y, Greven M, Kastner M A and Shirane G 1993 *Z. Phys.* **91** 373
- [34] Boehm M, Coad S, Roessli B, Zheludev A, Zolliker M, Böni P, Paul D McK, Esaki H, Motoyama N and Uchida S 1998 *Europhys. Lett.* **43** 77
- [35] A recent inelastic neutron scattering experiment reveals that the magnetic scattering at the antiferromagnetic zone center is visible down to 3 meV and then merges with the elastic signal. From this it is concluded that any gap is less than 3 meV, Lake B, Notbohm S, Tennant D A, Perring T G, Krabbes G and Sekar C, unpublished.
- [36] Benner H and Boucher J. P. 1990 in *Magnetic Properties of Layered Transition Metal Compounds* ed L J de Jongh (Dordrecht: Kluwer, Dordrecht) p 323
- [37] Chakravarty S and Orbach R 1990 *Phys. Rev. Lett.* **64** 224
- [38] Eskes H and Jefferson J H, *Phys. Rev. B* 1993 **48** 9788
- [39] Harisson W A 1980 *Electronic Structure and the Properties of Solids. The Physics of the Chemical Bond* (San Francisco: W H Freeman and Company)
- [40] Sharma R R, *Phys. Rev. B* 1979 **19** 2813
- [41] Moriya T 1963 *J. Phys. Soc. Japan* **18** 516

- [42] Kochelaev B I, Kan L, Elschner B and Elschner S 1994 *Phys. Rev. B* **49** 13106
- [43] Kataev V, Rameev B, Büchner B, Hücker M and Borowski R 1997 *Phys. Rev. B* **55** R3394
- [44] Note that in contrast to CaCu₂O₃ narrow ESR signals from the impurity spin states have been observed at low T in the polycrystalline samples of the spin-gapped two-leg $S = 1/2$ -ladder SrCu₂O₃ in the frequency range 35 - 340 GHz. See, Schwenk H, König D, Sieling M, Schmidt S, Palme W, Lüthi B, Zvyagin S, Eccleston R S, Azuma M and Takano M 1997 *Physica B* **237-238** 115